Article:
Boschmans, J, Lemière, F and Sobott, F (2017) Analyzing complex mixtures of drug-like molecules: ion mobility as an adjunct to existing liquid chromatography-(tandem) mass spectrometry methods. Journal of Chromatography A, 1490. pp. 80-88. ISSN 0021-9673

https://doi.org/10.1016/j.chroma.2017.02.015

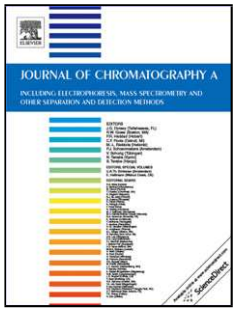

Title: Analyzing complex mixtures of drug-like molecules: ion mobility as an adjunct to existing liquid chromatography-(tandem) mass spectrometry methods

Authors: Jasper Boschmans, Filip Lemière, Frank Sobott

PII: S0021-9673(17)30238-8
DOI: http://dx.doi.org/doi:10.1016/j.chroma.2017.02.015
Reference: CHROMA 358285

To appear in: *Journal of Chromatography A*

Received date: 29-8-2016
Revised date: 24-1-2017
Accepted date: 9-2-2017

Please cite this article as: Jasper Boschmans, Filip Lemière, Frank Sobott, Analyzing complex mixtures of drug-like molecules: ion mobility as an adjunct to existing liquid chromatography-(tandem) mass spectrometry methods, Journal of Chromatography A http://dx.doi.org/10.1016/j.chroma.2017.02.015

Analyzing complex mixtures of drug-like molecules: ion mobility as an adjunct to existing liquid chromatography-(tandem) mass spectrometry methods

Jasper Boschmans[1], Filip Lemière[1], Frank Sobott*[1,2,3]

[1]Biomolecular & Analytical Mass Spectrometry, Department of Chemistry, University of Antwerp, Groenenborgerlaan 171, 2020 Antwerp, Belgium.
[2]Astbury Centre for Structural Molecular Biology, University of Leeds, Leeds LS2 9JT, United Kingdom
[3]School of Molecular and Cellular Biology, University of Leeds, LS2 9JT, United Kingdom.

Address correspondence to: frank.sobott@uantwerp.be

Abstract

The use of traveling wave ion mobility mass spectrometry (TWIMS) is evaluated in conjunction with, and as a possible alternative to, conventional LC-MS(/MS) methods for the separation and characterization of drug-like compounds and metabolites. As a model system we use an *in vitro* incubation mixture of the chemotherapeutic agent melphalan, which results in more than ten closely related hydrolysis products and chain-like oligomers.
Ion mobility as a filtering tool results in the separation of ions of interest from interfering ions, based on charge state and shape/size. Different classes of chemical compounds often display different mobilities even if they show the same LC behavior – thereby providing an orthogonal separation dimension. Small molecules with identical or similar m/z that only differ in shape/size (e.g. isomers and isobars, monomers/dimers) can also be distinguished using ion mobility. Similar to retention times and mass-to-charge ratios, drift times are analyte-dependent and can be used as an additional identifier.
We find that the compound melphalan shows two different drift times due to the formation of gas-phase charge isomers (protomers). The occurrence of protomers has important implications for ion mobility characterization of such analytes, and also for the interpretation of their fragmentation behavior (CID) in the gas phase.

Keywords: LC-MS; Tandem MS; Ion mobility; Isomer separation; Protomers; Melphalan

Highlights

- Ion mobility is easily integrated in existing LC-MS methods without loss of information or increase in analysis time
- Post-acquistion charge-state filtering and extraction of otherwise hard to detect signals
- Rapid classification of analyte classes based on ion mobility behaviour (combination of size/shape and charge state)
- Resolution of overlapping signals in addition to or as a faster replacement of LC separation
- Detection of gas-phase charge site isomers (protomers) in ion mobility

1. Introduction

LC-MS/MS is one of the most powerful and favored analytical techniques for the analysis of small molecules in complex matrices. Nonetheless, the analysis of samples containing co-eluting compounds and analytes with similar or identical MS properties (mass, fragmentation and/or isotope patterns) remains a frequent challenge. One of the breakthrough analytical technologies in the last decade is ion mobility-mass spectrometry (IM-MS) [1-3]. As a gas-phase separation technique, IM characterizes ions based on their collision cross-section (CCS; a parameter related to the ion's rotationally averaged size, shape, total charge and charge distribution). An acceleration voltage is applied along the ion's flight path through the drift cell filled with neutral buffer gas [4]. Due to friction, i.e. collisions with the gas molecules, the ions reach a characteristic velocity, and the time it takes for an ion to pass through the cell is called the drift time (t_d). The type of drift gas used, typically He or N_2, has a significant effect on the resolving power of ion mobility [5,6]. Moreover, the use of polarizable drift gases (e.g. N_2 or CO_2) can lead to separation of charge site isomers, i.e. (de)protomers, of an otherwise identical analyte molecule (see below).
Ion mobility itself has proven to be effective e.g. for detection of narcotics and explosives [7,8]. Although its hyphenation with MS in commercial instrumentation is a more recent development, it has already created new possibilities for the characterization of some classes of small molecules and metabolites [9-11]. Specific examples are the separation of isomeric disaccharides [12-14] and metal(-ligand) complexes [15-17] or the characterization of carbohydrate, glycan and lipid structures [18-23]. Particular interest recently focused on the phenomenon of alternative charge sites in small molecules that are observed in the gas phase, i.e. the observation of protonation site isomers (protomers) [24-26]. The routine use as a separation technique is however still in its infancy, and the added benefit (if any) of combining IM with LC-MS/MS has not been studied systematically. Here we utilize traveling wave ion mobility spectrometry (TWIMS), which has been described previously [27-29].

An important application of TWIMS in the context of complex samples is background filtering. Often samples contain unwanted additives such as salts, plasticizers or interfering analytes that hinder the detection of the compounds of interest. Even though ion suppression may still occur in the electrospray process, IM-MS can reveal specific analyte ions which are present in the spectra but difficult to discern, by separating them from interfering background ions based on their charge and shape/size [30,31]. Such filtering can also be performed post-acquisition, provided that the data were recorded in ion mobility mode [32].
Given that LC separations have a timescale of minutes and time-of-flight (TOF) detection occurs in microseconds, IM is easily integrated with its millisecond regime without affecting the timescale of the existing LC-MS/MS method, by adding an extra, orthogonal separation dimension. Relatively few studies have been published on the use of LC-IM-MS/MS so far [33-38], but this number is expected to increase considerably in the next years. While retention time (t_R), drift time (t_d) and mass-to-charge (m/z) provide key analytical determinants (e.g. polarity, shape/size and mass), the characterization of compounds solely based on these parameters could lead to incorrect assignment, and is often considered insufficient in practice. Fragmentation by MS/MS on the other hand is generally employed to obtain structural information [39,40], and we also investigate its use here together with ion mobility analysis.

Recently IM-MS/MS has been used to enhance peptide detection [41], study the fragmentation patterns of drug metabolites [42] and (de-)protomers [24-26,43,44].

The present study focuses on the efficiency and versatility of ion mobility as an adjunct to LC-MS/MS methods, by using a model compound mixture with moderate analytical complexity. We previously investigated melphalan (L-phenylalanine mustard; see Figure 1), an alkylating agent which is used in the treatment of cancer [45,46]. Several studies have been published discussing its (pharmaco)kinetics, binding to DNA and proteins [47-50], and its clinical applications. In aqueous solution, melphalan forms two major hydrolysis products [51,52] *in vitro*, mono- and dihydroxy melphalan, as well as chain-like oligomers [53]. In total, more than ten closely related degradation products were characterized before (Table 1). Understanding the complexity of these drug-related compounds is essential for our ability to accurately determine drug levels in patients, and particularly also for the quantitation of the active form of the drug in different sample matrices.

2. Materials and methods

Caution: melphalan, degradation products and oligomers are carcinogenic and should be handled with care.

2.1 Chemicals

Melphalan (Mel; min. 95 %) and sodium formate (HPLC, > 99.0 %) were purchased from Sigma – Aldrich (Bornem, Belgium). Acetonitrile (ACN; HPLC grade for gradient analysis) and formic acid (FA; 99+ %) were obtained from Acros (Geel, Belgium). Reverse osmosis (RO) water was prepared using a Silex water filtering system from Eurowater (Nazareth-Eke, Belgium). Leucine Enkephalin (Leu-Enk) was obtained from Waters (Manchester, UK).

2.2 Incubation of melphalan

A 1 mg/mL solution of Mel was prepared using RO water, and vortexed and sonicated to improve solubility. This solution was incubated at 37 ˚C for 3 h using a Thermomixer (Eppendorf, type 5436). Samples were centrifuged for 4 minutes at 14.000 rpm (Eppendorf miniSpin plus) to remove particles.
For direct infusion experiments, the sample was diluted 1:1 with a 50:50 ACN:RO (0.1% formic acid; FA) solution.

2.3 Instrumentation

2.3.1 nanoAcquity UPLC

A binary gradient was developed on a Waters nanoAcquity UPLC system (Milford, MA, USA). Trapping column: 180 µm x 20 mm; 5 µm Symmetry C_{18}; analytical column: 100 µm x 100 mm; 1.7 µm Acquity BEH130 C_{18} column (both Waters; Manchester, UK). Column temperature was kept at 30 ˚C. The gradient method used acidified H_2O (solvent A; 0.1 % FA) and ACN (solvent B) for analysis as well as for wash purposes. The gradient had a run time of 35 minutes, starting with 1.00 minute of on-column focusing. The gradient went from 1 to 50% B over 5.00 minutes, followed by 0.99 minutes of washing (99 % B) and 24 minutes of equilibration at initial conditions. Injection: 5 µL full loop (overfill factor 1).

2.3.2 Synapt G2 HDMS

In this study we used a Waters Synapt G2 HDMS mass spectrometer equipped with TWIMS technology. The TWIMS cell is located after the quadrupole (Q), between two collision cells (trap and transfer cell) and before the TOF [29]. Key features of this setup are the possibility to select a precursor ion in the quadrupole, perform collision-induced dissociation (CID) either prior to or post-IM-MS separation, and detect the accurate masses of the (fragment) ions in the TOF.

A chip-based NanoMate source (Advion, Ithaca, NY, USA) was used for positive ESI. The NanoMate was connected with the nanoAcquity pump using an LC-coupler. A spray voltage of 1.7 kV was applied. Source and desolvation temperatures were 80 and 60 °C respectively. For direct infusion experiments, a source temperature of 60 °C was used. Prior to the experiments, the instrument was calibrated for the appropriate mass range using sodium formate solution. In addition, for some experiments a solution of Leu-Enk was sprayed using a dual spray setup, and mass spectra were corrected by using the Leu-Enk (m/z 556.2771) signal as lock mass.

The parameters for the experiments without IM are: resolution mode, m/z range of 50-700, sample and extractor cone voltage of 25 V and 3 V, trap bias of 2 V, trap and transfer CE of 4 V and 0 V, respectively. The parameters for the experiments with IM are: resolution mode, m/z range of 50-600, 500-600 or 50-1000, sample cone voltage of 20-40 V, extraction cone voltage of 3 V, trap bias of 40-45 V, IMS wave velocity of 500-1400 m/s, IMS wave height of 40 V, He and IMS (N_2) gas flow of 180 mL/min and 90-100 mL/min, trap and transfer CE of 4 V and 0 V. Scan time: 1.0 sec for direct infusion and 0.500 sec for LC-coupling experiments. Interscan time: 0.024 sec.

2.4 Data acquisition

Data is acquired in multiple dimensions: LC, IM, MS and MS/MS, and for the purpose of this study extracted and displayed in 2 dimensions. Although several combinations are possible, the most relevant is IM/MS, next to LC/MS and LC/IM. Figure 1 visualizes the data acquisition for an LC-IM-MS/MS experiment.

For post-acquisition data filtering, a melphalan incubation sample is directly infused into the mass spectrometer without inclusion of an LC separation step. The separation in the TWIMS cell was optimized to give transmission for a wide m/z range. This allows detecting melphalan monomers, dimers and trimeric compounds. Data acquisition times, after optimization, are less than 5 minutes per sample.

Ion mobility vs. m/z data were exported to MassLynx without prior specific mass, charge or drift time selection (unless stated otherwise). In MassLynx, sequential m/z and t_d “filters” are applied which enable more targeted data extraction in the dimensions of interest. Practically, peaks in the mass spectrum or drift time plot are selected at FWHM, i.e. extracted drift time and m/z profiles are corresponding to the upper half around the apex of those peaks.

Isomer separation experiments comprise: the injection of the incubation mixture of melphalan, an LC separation using (nano)UPLC, IM separation and high-resolution MS detection. IM-MS parameters are fine-tuned for specific sets of ions (e.g. isomers) with the aim to obtain baseline-separated peaks in ion mobility. Driftscope software is used to extract and export the drift time plot accounting for all ions which elute at a given retention time.

3. Results and discussion

3.1 Post-acquisition data filtering

In a first set of experiments, we investigate the advantages of ion mobility for the separation of complex mixtures without the use of LC. Data analysis comprises the use of DriftScope software to plot drift times (t_d) vs. m/z values (see Figure 2; centre) and create an ion mobility plot. This representation is suitable for obtaining an overview of the types of analytes present and to discover trends in the acquired data. Grouped signals (i.e. within ellipses) represent ions with similar characteristics (mass, shape/size and charge). Exporting signals within these ellipses together with their underlying drift times results in spectra with specific charge states, as demonstrated in Figure 2a-d. Singly and doubly charged ions can easily be distinguished (Figures 2a and 2b). Based on their mass and isotope pattern, singly charged signals can be assigned to monomers (see Figure 2a) as well as di- and trimers (i.e. melphalan oligomers; see Figures 2c and d). For the doubly charged ions, oligomers from di- up to hexamers are observed.

When comparing the extracted mass spectrum of drift-time selected 2+ ions with the original, complete spectrum (data not shown but similar to Figure 2a), the signal intensity of the doubly charged ions appears enhanced (see Figure 2b) as the much stronger singly charged ions are now filtered out. Similarly, the signal-to-noise ratio of singly charged dimers and trimers appears greatly improved after selection of their signals in the 2D IM plot (enhanced spectra in Figure 2c and d; extracted from the 1+ ellipse in the center plot), demonstrating the power of ion mobility data filtering for targeted analyses.

A more detailed analysis of the ion mobility data (see Figure 3; zoom from Figure 2) shows three drift time signals at the same m/z 269: 2.66 ms, 3.15 ms and 3.90 ms. The complete drift time trace is indicated as a dotted line (left, vertical panel), while the superimposed colored profiles show the individual, extracted drift times. The signal at 3.90 ms accounts for a singly charged ion with m/z 269.1584, which can be assigned to the DOH monomer (M3). The two low-intensity signals at 2.66 ms (N3) and 3.15 ms ($M5_{a/b}$) are identified as 2+ ions based on their isotope patterns (data not shown), but being at m/z 269 they must also be dimeric. These doubly charged dimers show significantly different gas-phase characteristics (e.g. shape or size), and are therefore mobility-resolved. Similar observations were made for the other doubly charged dimers (see Table 1). We previously discovered the existence of nine unique dimeric compounds [53], which can be categorized into two classes: M-type and N-type dimers, with the N-type dimers formed after elimination of water from an M-type analogue. These data highlight how ions with very similar m/z values can have distinctly different associated ion mobility signals, facilitating their separation and identification.

3.2 Isomer separation

The main goal in the second set of experiments is to compare the performance of LC with IM separation for specific sets of ions (e.g. isomers). Previously, an LC-MS/MS method was developed to analyze the complex mixture of isomeric and isobaric melphalan-derived compounds. Baseline separation was achieved then for all compounds using (nano-)UPLC, and both MS/MS experiments and accurate mass determination were used for their identification [53]. With IM-MS implemented here in

a “panoramic” mode to cover species up to dimers, all ions in the acquired m/z-range are equally transmitted and detected in the mass spectrometer; but the settings do not yield the best possible IM resolution for each individual species.
Since the resolving power of the LC and IM methods is of particular interest here, we focus on compounds with the same nominal or exact masses, which pose the biggest analytical challenge. The separation of three singly charged melphalan dimers at m/z 537 ($M5_{a/b}$ and N3; see Figure 3 and 4a) is an interesting example. Extracting the drift time profile of each compound and their superposition reveals only minor differences (Figure 4b-c). Two singly charged, isobaric ions ($M5_b$ and N3) show virtually identical ion mobility behavior, whereas the third ion ($M5_a$), which is an isomer of $M5_b$, appears at a slightly longer drift time. In this case, ion mobility alone is only able to separate one of the isomers from the other two ions, whereas LC was able to separate all three from each other. The series of doubly charged $[M+2H]^{2+}$ and $[N+2H]^{2+}$ ions in Figure 2 (red/white dots in the 2+ ellipse) on the other hand, which also contains the $M5_{a/b}$ and N3 isomer/isobar pairs, are all drift-time separated. Tintaru *et al.* made a similar observation for poly(amidoamine) dendrimers [54], that a higher charge state may allow for better IM separation when compared to the singly charged ions. Development of a targeted method, which aims to replace LC with IM separation should therefore include higher charge states of the analyte.

3.3 Observation of multiple drift times for melphalan

During direct infusion IM-MS experiments, not one but two peaks are observed in the ion mobility spectrum for melphalan (m/z 305; see Figure 1 and 3). Both ions appear at m/z 305.0824, with drift times of 4.18 ms and 4.61 ms respectively. On the other hand, LC separation results in only one retention time for this molecule (see Figure 1). Analysis of a melphalan sample using ^{1}H-NMR reveals no major impurities (data not shown) that could cause a second drift time to be observed for m/z 305. This indicates that in solution only one form (e.g isomer) of melphalan is likely to be present. Therefore, the presence of a second drift time must be inherent to the gas-phase properties of the molecule and/or the ion mobility separation itself.
A study by Kaufmann *et al.* [55] reports on the existence of two ion types for the pesticide norfloxacin. These ‘isobaric ions’ have identical retention times and exact masses, but appear to have different gas-phase properties. Based on IM and MS/MS data, they conclude that these ions only differ in the site of protonation, and are thus referred to as ‘protomers’. Other studies have reported on the observation of protomers for different analytes using both MS as well as other techniques such as gas-phase infrared photodissociation (IRPD) spectroscopy [56-58]. We also explain the observation here of two drift times for melphalan by the presence of charge isomers (protomers) in the gas phase [26].

3.4 Structure assignment using MS/MS

While compounds can in many cases be identified based on their retention time (LC) or drift time (IM), the characterization of (unknown) structures requires MS/MS fragmentation data. MS/MS can be performed either in the trap and transfer cell of the instrument, before and after ion mobility separation, respectively. Transfer CID spectra of melphalan are shown in Figure 1, and a corresponding ion mobility plot-like visualization for the two melphalan protomers is given in Figure 5. The fragment ions are drift time-aligned here, since they originate from different, mobility-resolved precursor ions. These data show that both types of melphalan ions (protomers) have unique and characteristic fragmentation patterns. Most fragment ions are observed

at the drift time of the slower ion (4.61 ms), which is more easily fragmented. Characteristic for this drift time is the loss of NH_3, which generates a fragment ion at m/z 288, and also hints at -NH_2 protonation for this protomer. The faster ion (4.18 ms) results in fewer fragments, with a unique ion observed at m/z 168. This protomer represents melphalan protonation on the second nitrogen atom on the mustard side (see structures in Figure 5).
In contrast, "normal" CID spectra which are recorded without, or prior to, ion mobility separation (e.g. trap CID) contain fragments from both protomers together, i.e. they show a weighted sum of the fragmentation spectra for each of the two protomer ions (also see Figure 5). As the experimental parameters of electrospray ionization as well as the sampling interface ("source") are major factors in the formation of alternate protonation isomers, the relative abundance of protomers and the corresponding fragment intensities in CID will appear to be quite variable, precluding the use of MS/MS spectral libraries.

4. Conclusions and Outlook

Here we investigate the complementarity of LC and IM for the study of drug-like compounds, and show the benefits and limitations of adding ion mobility to the LC-MS/MS method toolbox; with an emphasis on how it can improve data quality and information content of complex samples. *In vitro* incubation samples of the alkylating agent melphalan result in complex spectra of ions with different charge states and overlapping isotopic and fragmentation patterns. We show that the addition of IM improves and simplifies the acquired data and enables post-acquisition data filtering. Data that have been acquired in mobility mode, but not analyzed in that dimension, can still be re-analyzed later should interferences become apparent.
While leaving the ESI process unaffected, ion mobility can overcome issues of overlapping peaks by adding an orthogonal separation. It also enables improved data visualization, resulting in cleaner and more information-rich MS spectra. Ion mobility is used here for charge-state filtering and the separation of different groups of compounds. By enabling software-based filtering of ions with distinct drift times or drift time ranges, IM-MS simplifies the interpretation of the mass spectra. Visualizing these data in a 2D ion mobility plot facilitates the observation of different molecular classes and functional groups. Since electrospray ionization (ESI) can generate multiply charged ions, overlapping mono- and oligomer peaks at the same m/z result in complex and only partly resolved mass spectra. Without the use of an additional separation step (e.g. ion mobility), interpretation of LC-MS data can be difficult due to overlapping isotope and fragmentation patterns and the wide concentration range of the analytes.

Unexpectedly, two drift times are observed for singly charged melphalan (m/z 305). The two species are only visible using IM-MS, and drift time-aligned fragmentation experiments give insight into their structural properties. We explain these findings with the presence of protonation site isomers (protomers), which originate from the ionization and desolvation process in the interface of the instrument, and therefore have no physiological relevance as a functional analyte. Protomer separation is thought to be the result of interactions between the dipole moment of the ion, resulting from its charge distribution, and polarizable gas molecules, which lead to an

additional retardation of ion movement through the drift gas [43,44,55,59]. A more detailed study of melphalan protomers has been published recently [26].
The possibility of alternative protonation forms is relevant for all LC analyses, which use MS/MS detection. Protomers are produced in the ESI source with varying intensities according to the parameters used, but only become visible in combination with IM. As they also fragment differently, this leads to somewhat unpredictable variations in fragment intensities, and is one important reason why ESI CID spectral libraries (similar to EI fragmentation libraries standardized at 70eV) are not popular.

Due to the potential of saving considerable analysis time, it could be advantageous to substitute LC with IM separation. Our data show that care should be taken though, as isobaric melphalan dimers are only partially drift-time resolved as 1+ ions, while the 2+ ions on the other hand can be separated by direct infusion IM-MS. As ESI usually produces more than one charge state, at least for larger analytes, a targeted IM-MS method utilizing higher charge states may well be able to replace LC-MS in some cases. The separation power of IM-MS is highly dependent on the physico-chemical properties of the analytes, particularly their size/shape or compactness ("density"). Using the current methods and/or technologies, baseline ion mobility separation could not be achieved here for some closely related compounds (e.g. 1+ melphalan dimers, isomers and isobars). Hence, the resolving power of the LC separation is still essential. For now, we are convinced that LC and IM should be regarded as complementary separation technologies. Ion mobility alone should not (yet) be seen, at the current resolving power ($dt_d/\Delta dt_d$) of 40 or less, as a faster substitute for liquid chromatography.

Nonetheless, the addition of IM to an existing LC-MS(/MS) method increases sample information and confidence of analyte identification significantly. MS/MS is essential to identify unknown compounds and to obtain important structural information, but baseline LC and/or IM separation of individual species should be achieved. The possibility to perform LC and IM separations orthogonally, either separately or in combination, is a major advantage over the current LC-MS and MS/MS approaches. Also, the IM-Q-TOF setup offers new possibilities for precursor-selective MS/MS, such as the ability to perform drift time-aligned fragmentation in the transfer cell of the instrument. Precursor ions are fragmented simultaneously and corresponding fragments identified based on their drift time, which they share with the precursor, instead of sequential mass-to-charge (i.e. quadrupole) selection of all ions of interest. Since no ions are lost during ion mobility separation, the data can be recorded in ion mobility mode and re-analyzed at a later stage when focusing on new compounds in the already recorded sample (e.g. drugs of abuse). As a result of this drift time-based selection, the method is also faster than sequential m/z selection using a quadrupole. Other drift gases can be used to increase the IM separation, similar to the use of LC columns with different stationary phases. New types of mobility analyzers (high-pressure multiplexed drift tubes and trapped ion mobility in funnels) are also now becoming available commercially, with a resolving power of up to 400. We are convinced that the addition of ion mobility separation will prove useful for the analysis of many complex mixtures of small molecules. The full power of an LC-IM-MS/MS approach will be developed in future work.

Acknowledgements

We would like to thank the Rosa Blanckaert Foundation and the Hercules Foundation for financial support and funding of the Synapt mass spectrometer. We thank Esther Marie Martin for helpful and critical comments on this manuscript.

References

[1] F. Lanucara, S.W. Holman, C.J. Gray, C.E. Eyers, The power of ion mobility-mass spectrometry for structural characterization and the study of conformational dynamics, Nat. Chem. 6 (2014) 281–249.

[2] A. Konijnenberg, A. Butterer, F. Sobott, Native ion mobility-mass spectrometry and related methods in structural biology, BBA - Proteins and Proteomics. 1834 (2013) 1239–1256.

[3] C. Lapthorn, F. Pullen, B.Z. Chowdhry, Ion mobility spectrometry-mass spectrometry (IMS-MS) of small molecules: Separating and assigning structures to ions, Mass. Spectrom. Rev. 32 (2012) 43–71.

[4] H.H. Hill Jr, W.F. Siems, R.S. Louis, Ion mobility spectrometry, Anal. Chem. 21 (1990) 321–355.

[5] P.M. Lalli, Y.E. Corilo, M. Fasciotti, et al., Baseline resolution of isomers by traveling wave ion mobility mass spectrometry: investigating the effects of polarizable drift gases and ionic charge distribution, J. Mass Spectrom. 48 (2013) 989–997.

[6] M.D. Howdle, C. Eckers, A.M.F. Laures, C.S. Creaser, The effect of drift gas on the separation of active pharmaceutical ingredients and impurities by ion mobility-mass spectrometry, Int. J. Mass Spectrom. 298 (2010) 72–77.

[7] G.R. Asbury, J. Klasmeier, H.H. Hill, Analysis of explosives using electrospray ionization/ion mobility spectrometry (ESI/IMS), Talanta. 50 (2000) 1291–1298.

[8] R. Fernández-Maestre, H.H. Hill, Ion mobility spectrometry for the rapid analysis of over-the-counter drugs and beverages, Int. J. Ion Mobil. Spectrom. 12 (2009) 91–102.

[9] L. Ahonen, M. Fasciotti, G.B.A. Gennäs, et al., Separation of steroid isomers by ion mobility mass spectrometry, J. Chrom. A. 1310 (2013) 133–137.

[10] M. Benassi, Y.E. Corilo, D. Uria, R. Augusti, M.N. Eberlin, Recognition and resolution of isomeric alkyl anilines by mass spectrometry, J. Am. Soc. Mass Spectrom. 20 (2009) 269–277.

[11] S. Crotty, S. Gerişlioğlu, K.J. Endres, C. Wesdemiotis, U.S. Schubert, Polymer architectures via mass spectrometry and hyphenated techniques: A review, Anal. Chim. Acta. 932 (2016) 1–21.

[12] M. Fasciotti, G.B. Sanvido, V.G. Santos, P.M. Lalli, M. McCullagh, G.F. de Sá, et al., Separation of isomeric disaccharides by traveling wave ion mobility mass spectrometry using CO2 as drift gas, J. Mass Spectrom. 47 (2012) 1643–1647.

[13] M.M. Gaye, R. Kurulugama, D.E. Clemmer, Investigating carbohydrate isomers by IMS-CID-IMS-MS: precursor and fragment ion cross-sections, Analyst. 140 (2015) 6922–6932.

[14] Y. Huang, E.D. Dodds, Ion-neutral collisional cross sections of carbohydrate isomers as divalent cation adducts and their electron transfer products, Analyst. 140 (2015) 6912–6921.

[15] J.P. Williams, J.M. Brown, I. Campuzano, P.J. Sadler, Identifying drug metallation sites on peptides using electron transfer dissociation (ETD), collision induced dissociation (CID) and ion mobility-mass spectrometry (IM-MS), Chem. Commun. 46 (2010) 5458.

[16] J.P. Williams, T. Bugarcic, A. Habtemariam, K. Giles, I. Campuzano, P.M.

Rodger, et al., Isomer separation and gas-phase configurations of organoruthenium anticancer complexes: Ion mobility mass spectrometry and modeling, J. Am. Soc. Mass Spectrom. 20 (2009) 1119–1122.
[17] V.E. Wright, F. Castro-Gómez, E. Jurneczko, J.C. Reynolds, A. Poulton, S.D.R. Christie, et al., Structural studies of metal ligand complexes by ion mobility-mass spectrometry, Int. J. Ion Mobil. Spec. 16 (2013) 61–67.
[18] H. Li, B.K. Bendiak, W.F. Siems, D.R. Gang, H.H. Hill Jr., Carbohydrate Structure Characterization by Tandem Ion Mobility Mass Spectrometry (IMMS), Anal. Chem. 85 (2013) 2760–2769.
[19] L.S. Fenn, J.A. McLean, Structural resolution of carbohydrate positional and structural isomers based on gas-phase ion mobility-mass spectrometry, Phys. Chem. Chem. Phys. 13 (2011) 2196–2205.
[20] K. Pagel, D.J. Harvey, Ion mobility–mass spectrometry of complex carbohydrates: collision cross sections of sodiated N-linked glycans, Anal. Chem. 85 (2013) 5138–5145.
[21] J. Hofmann, H.S. Hahm, P.H. Seeberger, K. Pagel, Identification of carbohydrate anomers using ion mobility-mass spectrometry, Nature. 526 (2015) 241–244.
[22] V. Steinmetz, G.L. Glish, P. Maitre, Probing Mobility-Selected Saccharide Isomers: Selective Ion–Molecule Reactions and Wavelength-Specific IR Activation, J. Phys. Chem. A. 119 (2015) 6057–6064.
[23] M. Kliman, J.C. May, J.A. McLean, Lipid analysis and lipidomics by structurally selective ion mobility-mass spectrometry, Biochim. Biophys. Acta. 1811 (2011) 935–945.
[24] R.S. Galaverna, G.A. Bataglion, G. Heerdt, G.F. de Sá, R. Daroda, V.S. Cunha, et al., Are Benzoic Acids Always More Acidic Than Phenols? The Case of ortho-, meta-, and para-Hydroxybenzoic Acids, Eur. J. Org. Chem. 2015 (2015) 2189–2196.
[25] S. Warnke, J. Seo, J. Boschmans, F. Sobott, J.H. Scrivens, C. Bleiholder, et al., Protomers of Benzocaine: Solvent and Permittivity Dependence, J. Am. Chem. Soc. 137 (2015) 4236–4242.
[26] J. Boschmans, S. Jacobs, J.P. Williams, M. Palmer, K. Richardson, K. Giles, et al., Combining density functional theory (DFT) and collision cross-section (CCS) calculations to analyze the gas-phase behaviour of small molecules and their protonation site isomers, Analyst. 141 (2016) 4044–4054.
[27] K. Giles, S.D. Pringle, K.R. Worthington, D. Little, J.L. Wildgoose, R.H. Bateman, Applications of a travelling wave-based radio-frequency-only stacked ring ion guide, Rapid Commun. Mass Spectrom. 18 (2004) 2401–2414.
[28] A.A. Shvartsburg, R.D. Smith, Fundamentals of Traveling Wave Ion Mobility Spectrometry, Anal. Chem. 80 (2008) 9689–9699.
[29] S.D. Pringle, K. Giles, J.L. Wildgoose, et al., An investigation of the mobility separation of some peptide and protein ions using a new hybrid quadrupole/travelling wave IMS/oa-ToF instrument, Int. J. Mass Spectrom. 261 (2007) 1–12.
[30] V. Domalain, V. Tognetti, M. Hubert-Roux, C.M. Lange, L. Joubert, J. Baudoux, et al., Role of Cationization and Multimers Formation for Diastereomers Differentiation by Ion Mobility-Mass Spectrometry, J. Am. Soc. Mass Spectrom. 24 (2013) 1437–1445.
[31] C. Eckers, A.M.F. Laures, K. Giles, H. Major, S. Pringle, Evaluating the utility

of ion mobility separation in combination with high-pressure liquid chromatography/mass spectrometry to facilitate detection of trace impurities in formulated drug products, Rapid Commun. Mass Spectrom. 21 (2007) 1255–1263.

[32] D.J. Harvey, C.A. Scarff, M. Edgeworth, et al., Travelling wave ion mobility and negative ion fragmentation for the structural determination of N-linked glycans, Electrophoresis. 34 (2013) 2368–2378.

[33] M.T. Jafari, K.L. Crowell, K.L. Crowell, T. Khayamian, E.S. Baker, E.S. Baker, et al., Increasing Confidence of LC-MS Identifications by Utilizing Ion Mobility Spectrometry, Int. J. Mass Spectrom. 354-355 (2013) 312–317.

[34] C. Chen, K. Hou, W. Wang, J. Li, H. Li, Ambient temperature nanoelectrospray ion mobility detector for high performance liquid chromatography in determining amines, J. Chromatogr. A. 1358 (2014) 192–198.

[35] J. Regueiro, A. Giri, T. Wenzl, Optimization of a Differential Ion Mobility Spectrometry–Tandem Mass Spectrometry Method for High-Throughput Analysis of Nicotine and Related Compounds: Application to Electronic Cigarette Refill Liquids, Anal. Chem. 88 (2016) 6500–6508.

[36] I. Márquez-Sillero, S. Cárdenas, M. Valcárcel, Determination of water-soluble vitamins in infant milk and dietary supplement using a liquid chromatography on-line coupled to a corona-charged aerosol detector, J. Chromatogr. A. 1313 (2013) 253-258.

[37] R.W. Smith, D.E. Toutoungi, J.C. Reynolds, A.W.T. Bristow, A. Ray, A. Sage, et al., Enhanced performance in the determination of ibuprofen 1-beta-O-acyl glucuronide in urine by combining high field asymmetric waveform ion mobility spectrometry with liquid chromatography-time-of-flight mass spectrometry, J. Chromatogr. A. 1278 (2013) 76–81.

[38] A. Malkar, N.A. Devenport, H.J. Martin, P. Patel, M.A. Turner, P. Watson, et al., Metabolic profiling of human saliva before and after induced physiological stress by ultra-high performance liquid chromatography–ion mobility–mass spectrometry, Metabolomics. 9 (2013) 1192–1201.

[39] H.H. Maurer, Multi-analyte procedures for screening for and quantification of drugs in blood, plasma, or serum by liquid chromatography-single stage or tandem mass spectrometry (LC-MS or LC-MS/MS) relevant to clinical and forensic toxicology, Clin. Biochem. 38 (2005) 310–318.

[40] F.W. McLafferty, Tandem mass spectrometry (MS/MS): a promising new analytical technique for specific component determination in complex mixtures, Accounts Chem. Res. 13 (1980) 33–39.

[41] L.J. Brown, R.W. Smith, D.E. Toutoungi, J.C. Reynolds, A.W.T. Bristow, A. Ray, et al., Enhanced analyte detection using in-source fragmentation of field asymmetric waveform ion mobility spectrometry-selected ions in combination with time-of-flight mass spectrometry, Anal. Chem. 84 (2012) 4095–4103.

[42] F. Cuyckens, C. Wassvik, R.J. Mortishire-Smith, G. Tresadern, I. Campuzano, J. Claereboudt, Product ion mobility as a promising tool for assignment of positional isomers of drug metabolites, Rapid Commun. Mass Spectrom. 25 (2011) 3497–3503.

[43] P.M. Lalli, B.A. Iglesias, H.E. Toma, G.F. Sa, R.J. Daroda, J.C. Silva Filho, et al., Protomers: formation, separation and characterization via travelling wave ion mobility mass spectrometry, J. Mass Spectrom. 47 (2012) 712–719.

[44] C. Lapthorn, T.J. Dines, B.Z. Chowdhry, et al., Can ion mobility mass

spectrometry and density functional theory help elucidate protonation sites in “small” molecules? Rapid Commun. Mass Spectrom. 27 (2013) 2399–2410.
[45] P.E. Van Schil, J.M. Hendriks, B.P. van Putte, B.A. Stockman, P.R. Lauwers, P.W. ten Broecke, et al., Isolated lung perfusion and related techniques for the treatment of pulmonary metastases, Eur. J. Cardiothorac. Surg. 33 (2008) 487–496.
[46] W.A. den Hengst, J.M.H. Hendriks, B. Balduyck, et al., Phase II Multicenter Clinical Trial of Pulmonary Metastasectomy and Isolated Lung Perfusion with Melphalan in Patients with Resectable Lung Metastases, J. Thorac. Oncol. 9 (2014) 1547–1553.
[47] B. Van den Driessche, E. Esmans, A. Van der Linden, W. Van Dongen, E. Schaerlaken, F. Lemiere, et al., First results of a quantitative study of DNA adducts of melphalan in the rat by isotope dilution mass spectrometry using capillary liquid chromatography coupled to electrospray tandem mass spectrometry, Rapid Commun. Mass Spectrom. 19 (2005) 1999–2004.
[48] M.H.N. Tattersall, M. Jarman, E.S. Newlands, L. Holyhead, R.A.V. Milstead, A. Weinberg, Pharmaco-kinetics of melphalan following oral or intravenous administration in patients with malignant disease, Eur. J. Cancer (1965). 14 (1978) 507–513.
[49] V.R. Thompson, A.P. DeCaprio, Covalent Adduction of Nitrogen Mustards to Model Protein Nucleophiles, Chem. Res. Toxicol. 26 (2013) 1263–1271.
[50] D. Dewaele, F. Sobott, F. Lemière, Covalent adducts of melphalan with free amino acids and a model peptide studied by liquid chromatography/tandem mass spectrometry, Rapid Commun. Mass Spectrom. 30 (2016) 719–730.
[51] A.G. Bosanquet, Stability of melphalan solutions during preparation and storage, J. Pharm. Sci. 74 (1985) 348–351.
[52] G. De Boeck, K. Van Cauwenberghe, A. Eggermont, A. Van Oostertom, E. de Bruijn, Determination of melphalan and hydrolysis products in body fluids by GC-MS, J. High Res. Chromatogr. 20 (1997) 697–700.
[53] J. Boschmans, E. De Bruijn, P. Van Schil, F. Lemière, Analysis of novel melphalan hydrolysis products formed under isolated lung perfusion conditions using liquid chromatography/tandem mass spectrometry, Rapid Commun. Mass Spectrom. 27 (2013) 835–841.
[54] A. Tintaru, S. Pricl, L. Denbigh, X. Liu, L. Peng, L. Charles, Conformational changes of small PAMAM dendrimers as a function of their charge state: A combined electrospray mass spectrometry, traveling-wave ion mobility and molecular modeling study, Int. J. Mass Spectrom. 354-355 (2013) 235–241.
[55] A. Kaufmann, P. Butcher, K. Maden, et al., Are liquid chromatography/electrospray tandem quadrupole fragmentation ratios unequivocal confirmation criteria? Rapid Commun. Mass Spectrom. 23 (2009) 985–998.
[56] S.-W. Lee, H. Cox, W.A. Goddard, et al., Chemistry in Nanodroplets: Studies of Protonation Sites of Substituted Anilines in Water Clusters Using FT-ICR, J. Am. Chem. Soc. 122 (2000) 9201–9205.
[57] T.M. Chang, J.S. Prell, E.R. Warrick, E.R. Williams, Where’s the Charge? Protonation Sites in Gaseous Ions Change with Hydration, J. Am. Chem. Soc. 134 (2012) 15805–15813.
[58] J. Schmidt, M.M. Meyer, I. Spector, et al., Infrared Multiphoton Dissociation Spectroscopy Study of Protonated p-Aminobenzoic Acid: Does Electrospray Ionization Afford the Amino- or Carboxy-Protonated Ion? J. Phys. Chem. A.

115 (2011) 7625–7632.
[59] J.L. Campbell, J.C.Y. Le Blanc, B.B. Schneider, Probing electrospray ionization dynamics using differential mobility spectrometry: the curious case of 4-aminobenzoic acid, Anal. Chem. 84 (2012) 7857–7864.

Figures

Figure 1
Visualization of an LC-IM-MS/MS experiment. Data is acquired in multiple dimensions: LC, IM, MS and MS/MS. LC peak and drift time profile are displayed for melphalan (M1; m/z 305) and the dimer M7 (m/z 573; for compound labels see Table 1). For melphalan, two different drift times are observed and each one results in a different MS/MS spectrum. In the CID spectrum of the t_d=4.61 ms species, the melphalan precursor ion is fully fragmented (no m/z 305 peak left; middle spectrum in right column).

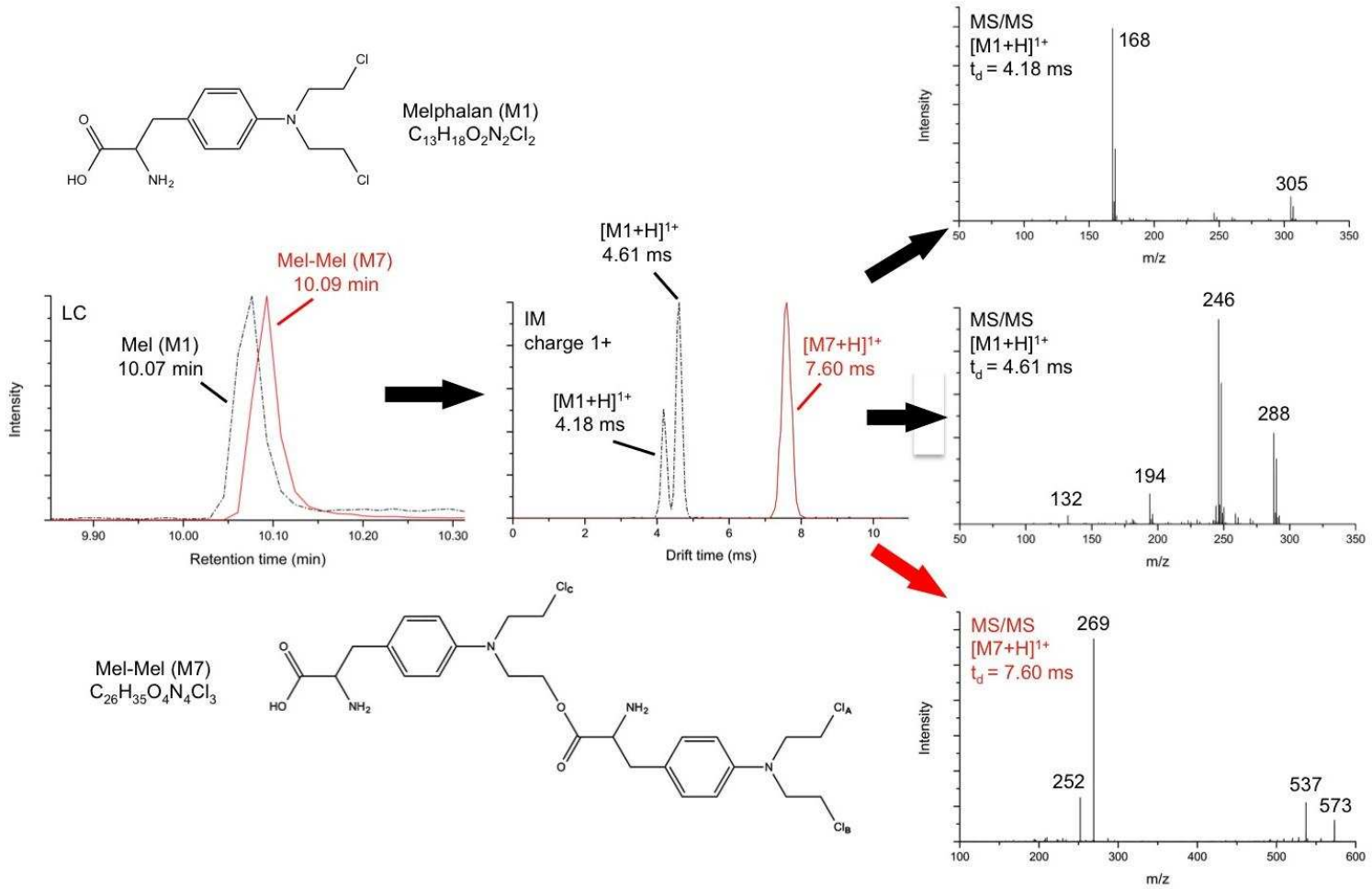

Figure 2
Ion mobility plot (centre) and extracted mass spectra for different charge states (a-b) and different melphalan oligomer sizes (c-d). The TIC mass spectrum looks similar to (a), as singly charged ions are observed as very intense signals while the higher charge states are at much lower intensity. IM separation and charge state extraction (b) results in better visualization of the 2+ ions (b). Two types of dimers are observed: the M-type (white dots) and N-type (red dots) dimers, which are formed after elimination of water from an M-type analogue. Both dimers are only separated as 2+ ions, but not as 1+ ions..

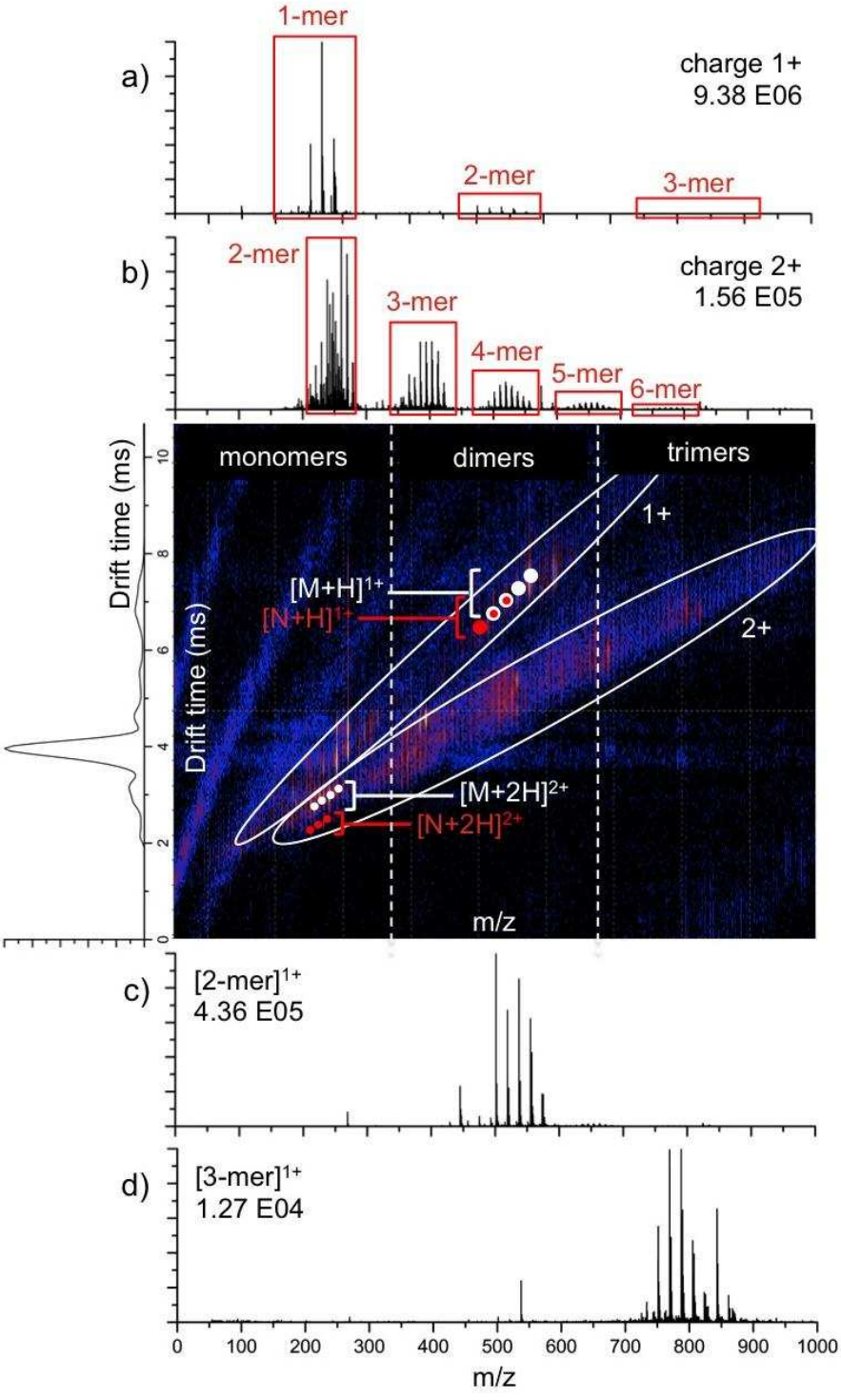

Figure 3
Enlarged section of the IM plot (Figure 2) with extracted drift times and m/z values for m/z 269 and m/z 305 ions (left panel). The dotted line represents the entire drift time spectrum, while individual signals are normalized to 100% intensity separately and shown superimposed in color. M-type ions are shown by white dots, N-type ions by red dots. The size of each dot gives an indication of the signal intensities.

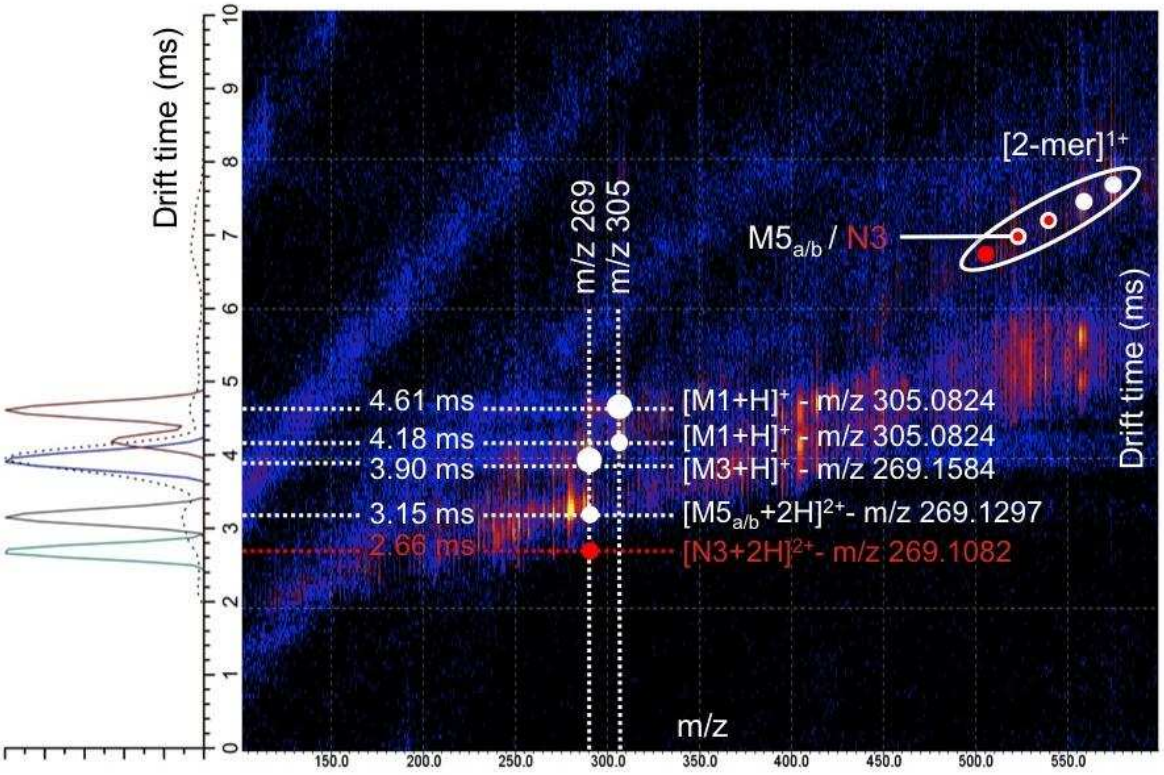

Figure 4
(a) Partial structures of the m/z 537 dimers from Figure 3 ($M5_{a/b}$ and N3). The subscript 'a/b' refers to the two observed isomers. Chemical formulae, retention times and drift times for the isobaric and isomeric compounds can be found in Table 1. (b) LC chromatogram and (c) superimposed drift time signals for the m/z 537 dimers, i.e. $M5_{a/b}$ and N3. Good LC separation is achieved for all compounds. After optimization of the IM parameters for this specific set of ions, only a partial IM separation is achieved for the $M5_a$ and $M5_b$ isomers.

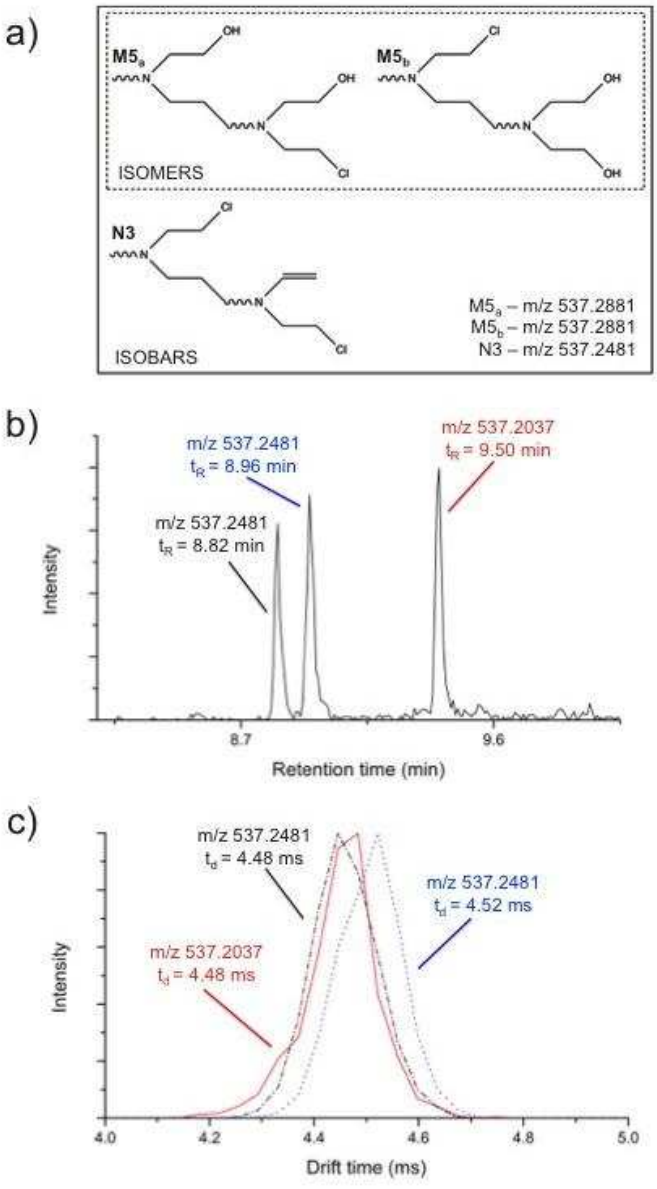

Figure 5
Ion mobility plot-like visualization of the fragmentation spectra for transfer CID experiments of melphalan. Each protomer is drift-time aligned and has a distinct fragmentation pattern with unique fragment ions (e.g. m/z 288 and m/z 168). The MS/MS data hint at -NH_2 protonation for the slower ion (t_d= 4.61 ms; black box) and protonation of the second nitrogen atom on the mustard moiety for the faster ion (t_d= 4.18 ms; red box). The MS/MS spectrum shows trap CID products of melphalan similar to those acquired on instruments lacking IM (e.g. tandem quadrupole MS).

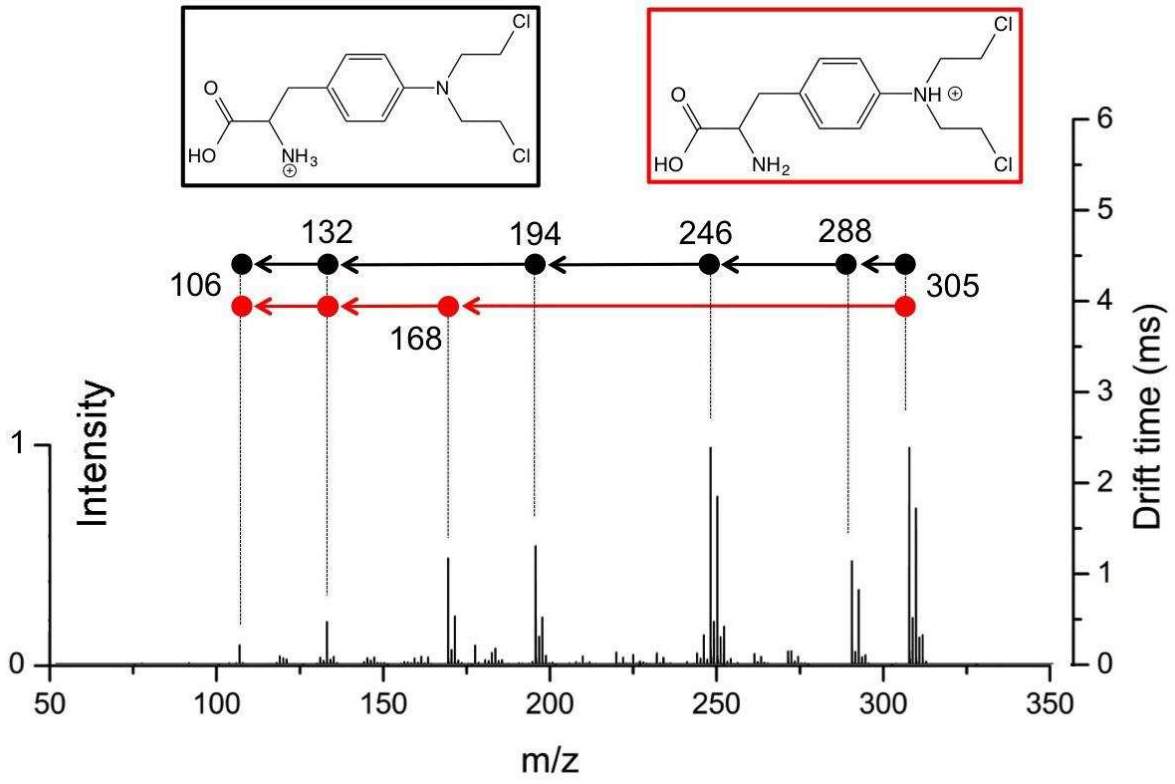

Table 1 Overview of the calculated ions that are expected for melphalan (M1) and its two monomeric hydrolysis products, monohydroxymelphalan (MOH; M2) and dihydroxymelphalan (DOH; M3), together with the dimeric compounds (M4-M7 and N1-N3).The subscript 'a/b' refers to the observed isomers (see Figure 5). Experimental CCS values are those of the singly charged ions.

Compound	Class	Chemical formula	Calculated m/z		Structural isomers	t_R (min)	t_d (ms)	
			$[M+H]^{1+}$	$[M+2H]^{2+}$			$[M+H]^{1+}$	$[M+2H]^{2+}$
M3	Monomer	$C_{13}H_{20}O_4N_2Cl_0$	269.1502	-	1	5.05	3.90	-
M2	Monomer	$C_{13}H_{19}O_3N_2Cl_1$	287.1163	-	1	8.95	4.07	-
M1	Monomer	$C_{13}H_{18}O_2N_2Cl_2$	305.0824	-	1	10.07	4.18 4.61	- -
N1	Dimer	$C_{26}H_{36}O_6N_4Cl_0$	501.2715	251.1396	1	8.54	6.56	2.55
N2	Dimer	$C_{26}H_{35}O_5N_4Cl_1$	519.2376	260.1227	1	9.05	6.78	2.60
M4	Dimer	$C_{26}H_{38}O_7N_4Cl_0$	519.2820	260.1449	1	8.36	6.78	3.04
N3	Dimer	$C_{26}H_{34}O_4N_4Cl_2$	537.2037	269.1058	1	9.50	7.05	2.66
$M5_{a/b}$	Dimer	$C_{26}H_{37}O_6N_4Cl_1$	537.2481	269.1280	2	8.82_b / 8.96_a	$7.05_{a/b}$	3.15
$M6_{a/b}$	Dimer	$C_{26}H_{36}O_5N_4Cl_2$	555.2142	278.1110	2	9.49_a / 9.66_b	$7.38_{a/b}$	3.20
M7	Dimer	$C_{26}H_{35}O_4N_4Cl_3$	573.1804	287.0941	1	10.09	7.60	3.36